processes

MDPI

Article

A Microgrid Simulation Platform Based on Cyber-Physical Technology

Dongli Jia [1], Xiaoyu Yang [1], Wanxing Sheng [1], Keyan Liu [1], Kaitong Yang [2,*], Xiaoming Li [2] and Weijie Dong [2]

[1] China Electric Power Research Institute Co., Ltd., Beijing 100192, China; jiadl@epri.sgcc.com.cn (D.J.); yangxiaoyu1@epri.sgcc.com.cn (X.Y.); wxsheng@263.net (W.S.); liukeyan@126.com (K.L.)
[2] College of mechanical and electrical engineering, Beijing Information Science and Technology University, Xiaoying Campus, Beijing 100196, China; lixiaoming8835@126.com (X.L.); dongweijie163@163.com (W.D.)
* Correspondence: ykt101010@163.com

Abstract: With the transformation of energy structure and the development of new power systems, higher requirements have been put forward for the performance and stability of microgrids. To adapt to the multi-information, multi-energy, and multi-business characteristics of microgrids, this paper proposes a cyber-physical system (CPS) based a microgrid simulation platform, which constructs an integration architecture composed of the physical system, main station system, and strategy simulation system. Through the interaction of information and energy businesses, real-time reproduction and state control of business scenarios are achieved. The platform innovatively introduces the theory of finite state machine (FSM) and designs a state transition strategy. Taking fault optimization as an example, the optimal path can be selected through state transition, and the system fault optimization effect is improved based on FSM. Compared to traditional methods, this platform reduces simulation time by 16% to 86.6%, significantly shortening scene reproduction time. In addition, the practical application value of the platform in fault optimization and operational efficiency improvement was verified by building a semi-physical simulation system based on a rapid control prototype (RCP) and hardware-in-the-loop testing (HIL).

Keywords: cyber-physical technology; microgrid; finite state machine; integrated simulation platform; fault optimization

check for updates

Academic Editor: Wen-Jer Chang

Received: 26 February 2025
Revised: 7 April 2025
Accepted: 14 April 2025
Published: 8 May 2025

Citation: Jia, D.; Yang, X.; Sheng, W.; Liu, K.; Yang, K.; Li, X.; Dong, W. A Microgrid Simulation Platform Based on Cyber-Physical Technology. *Processes* **2025**, *13*, 1441. https://doi.org/10.3390/pr13051441

Copyright: © 2025 by the authors. Licensee MDPI, Basel, Switzerland. This article is an open access article distributed under the terms and conditions of the Creative Commons Attribution (CC BY) license (https://creativecommons.org/licenses/by/4.0/).

1. Introduction

In recent years, the transformation of the global energy structure has become a core issue in promoting sustainable development. In order to implement the reform and reconstruction of the new power system in the context of "carbon peak and neutrality goals" [1], higher demands have been put forward for the performance and stability of the new power system [2]. Due to the greater precision and complexity of large-scale distributed renewable energy systems with flexible power equipment, and the uncertainty of new source load power, microgrids urgently require flexible and controllable power regulation and digital operation management methods [3]. Active hierarchical control of distributed energy resources increasingly relies on the coupling of power systems and CPS [4]. CPS, through information acquisition, data analysis, intelligent decision-making, and control, enables power systems to respond more efficiently to environmental changes and make real-time adjustments [5]. The integration of CPS technology, which combines computing, communication, and power systems to develop an integrated simulation platform for microgrids, is becoming increasingly valuable.

Microgrids based on information physics technology have become a new development trend, and some scholars have conducted related research. Reference [6] proposed a cross-sectional optimization (CSO) algorithm to solve parameter optimization problems and established a small-signal model for multi-source and multi-load microgrids. Reference [7] introduced a two-stage energy storage optimization method that comprehensively considers the reliability and economic efficiency of distribution networks. Based on the reliability model of power supply with a single primary source, energy storage power supply reliability models were developed for single-point and multi-point access structures. Reference [8] presented a fault location method based on the Beetle Swarm Optimization algorithm, analyzing the fault characteristics on the post-short-circuit side and establishing a mathematical model for fault location. While these studies independently examine energy and information, they do not address the coupled characteristics between energy and information.

The development of microgrid CPS is rapid, and the complexity of the system is increasing. The reliability of the physical system is increasingly dependent on the support of the information system. Therefore, it is increasingly important to conduct reliability analysis and evaluation of the system. Many experts and scholars have conducted research in this area. Reference [9] proposed a multi-source coordinated recovery method for distribution network CPS based on info-gap decision theory, incorporating post-disaster recovery models that account for network reconfiguration and uncertainties in renewable energy output. Reference [10] introduced a rapid recovery approach for microgrid power supply following CPS failures caused by extreme weather, using measures such as communication blind-zone clustering to simplify topology and network slicing for resource optimization. Reference [11] developed a reliability assessment model for distribution network CPS based on Generalized Stochastic Petri Nets (GSPNs), analyzing the impacts of information attacks and component failures, and combining maximum flow theory with dynamic inference to enhance evaluation efficiency by avoiding exhaustive analysis. Reference [12] proposes an FDIA detection method for power information physical systems based on ASR UFK and IMC prediction algorithms, which improves detection accuracy through state estimation and bias analysis. Reference [13] designed a CPS framework considering interdependence, leveraging complex network theory and applying structure- and function-based repair strategies to evaluate repair efficiency comprehensively. Reference [14] proposed a multi-stage coordinated recovery strategy for CPS failures caused by natural disasters, taking into account grid integration and interdependencies between systems, and assessing resilience metrics during the recovery process. Reference [15] utilized state machines at the physical device layer, expressed control decisions with tuples at the decision-making layer, and set optimization objectives at the system optimization layer, thereby constructing an integrated cyber-physical model that significantly enhanced the observability of microgrid systems. Reference [16] established a state probability model based on the Markov process Monte Carlo method to analyze the impact of information equipment failures on system reliability. However, Markov processes mainly target stochastic problems and have an insufficient ability to handle deterministic problems. Reference [17] proposed a multi-dimensional Q-V droop control method based on known information from normal nodes and the physical layer to mitigate the effects of communication disruptions, enabling precise voltage control and improving voltage regulation resilience. Reference [18] introduced a distribution CPS architecture based on event-driven models, designed a framework for information-physical cascading failure evolution mechanisms, and studied the importance of information nodes and the probability of successful attacks. Reference [19] employed predictive methods to identify and classify vulnerable generating units, ensuring transient stability while addressing the risks associated with the loss of network observability. Reference [20]

proposed an edge computing node deployment optimization method based on community theory, improving network stability and response speed by integrating power flow and line impedance. Reference [21] presented a local evolution model for communication networks based on the physical grid topology, analyzing the impact of reconnection probability on self-organizing states and cascading failures in power CPS, thereby enhancing the system's resistance to cascading failures. These studies focus on the optimization and recovery strategies of CPS, analyzing the coupling characteristics of distribution networks under various scenarios and the synergistic effects of multiple measures. It is evident that the integration of information flow and energy flow has become an inevitable trend in the development of modern microgrids. However, there remains a lack of systematic cyber-physical integration platforms that support simulation and analysis across diverse business applications.

In the analysis and control of microgrid state transitions, Reference [22] proposed a real-time scheduling anti-error control method for power systems. This method establishes an overall framework and model for scheduling anti-error control based on finite state machines. Reference [23] introduced a dual-vector model predictive control strategy, utilizing FSM to describe a finite control set and restricted vector switching, thereby simplifying the system design approach. Reference [24] presented an FSM-based modulation technique, applying it to a boost converter's modulation module to regulate output voltage stability. Reference [25] developed an FSM-based multi-flow integration simulation engine for distribution networks, constructing a real-time rapid simulation architecture with a state interaction control scheme between the physical layer, host layer, and real-time simulation layer. The above research demonstrates the application advantages of finite state machines in structure and dynamic transformation, which can provide theoretical support for the integration simulation platform of microgrids.

Based on the aforementioned research progress and analysis, this paper addresses the technical demands in the application of cyber-physical technology within microgrids and proposes a simulation platform and implementation scheme oriented towards business integration. The main contributions of this study are as follows:

(1) An architecture integrating cyber-physical technology and business applications is proposed. This architecture incorporates the physical system, the central station system, and the strategy simulation system. By leveraging the business query method of the central station system, real-time simulation of various business applications is achieved.

(2) An FSM model for the integrated simulation platform is developed. Through state division and transitions, the deep integration of the physical system, the central station system, and the strategy simulation system is realized, thereby enhancing simulation efficiency and business scenario reproduction capabilities.

The remainder of this paper is organized as follows: The Section 2 proposes a method for integrating cyber-physical technology with business applications in microgrids. The Section 3 constructs an integrated simulation platform based on finite state machines. The Section 4 analyzes the business state transition strategy and communication format, using fault optimization as an example. The Section 5 employs semi-physical simulation technology to replicate the fault optimization scenario and conducts an in-depth discussion of the simulation results. The Section 6 concludes the paper by summarizing the main findings of this research. The list of variables and terms mainly used in this paper is summarized in Table 1.

Table 1. Description of variables and technical terms.

	Symbol	Explanation
variables	S	Finite set of states
	C	Collection of events
	S_0	Initial state
	S_n	Target state
	f	State transition function
	S_i	Current state
	C_i	Current input event
	O_n	Output state
	g	Output function
	C_n	Set of output events
technical terms	C-ADMM-A	Alternating direction method of multiplier algorithm in classical computing environment, A stands for adaptive update with penalty factor
	C-ADMM-F	Alternating direction method of multiplier algorithm in classical computing environment, F stands for fixed penalty factor
	CADMM + SA	Simulated annealing algorithm for discrete problems in classical computing environment
	QA-ADMM-A-1	Quantum annealing embedded ADMM algorithm under a solver
	QA-ADMM-A-2	Quantum annealing embedded ADMM algorithm based on b solver

2. Microgrid CPS and Business Integration Methods

2.1. Cyber-Physical Technology

The microgrid is a multi-dimensional cyber-physical system (CPS) where continuous and discrete states coexist and interact. The application of cyber-physical technology meets the dynamic coupling state requirement of microgrids, while also addressing the real-time control and reliability needs of the system.

In the actual operation of a microgrid, the energy distribution (i.e., power flow distribution) reflects the operating status of the grid. Data acquisition devices collect parameter signals that represent the physical system's state and convert them into discrete digital signals. These digital signals are input into the information system, where they undergo communication, transformation, and computational processing to generate control instructions, which are then fed back into the physical system. As shown in Figure 1, the information system monitors energy information within the physical system, and the control instructions generated by the information system also influence the energy distribution within the physical system. In real-time simulation, monitoring and instruction information are exchanged and updated in real time, establishing a close relationship between the two.

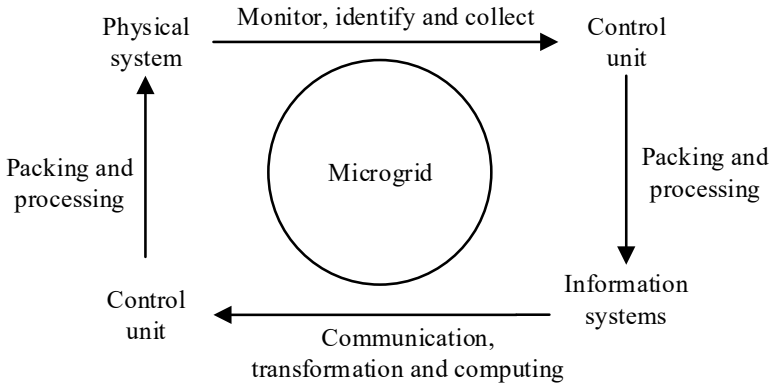


Figure 1. Cyber-physical technology coupling process.

2.2. CPS-Based Microgrid Simulation Platform

As shown in Figure 2, microgrid business applications include voltage quality, energy monitoring, operation status monitoring, fault location and optimization, availability monitoring, energy scheduling, system timing, and load control. These business applications continuously evolve during the operation of the microgrid. They may occur independently or simultaneously, and transition between each other in the form of the microgrid's operational state, thereby forming the operational framework of the microgrid.

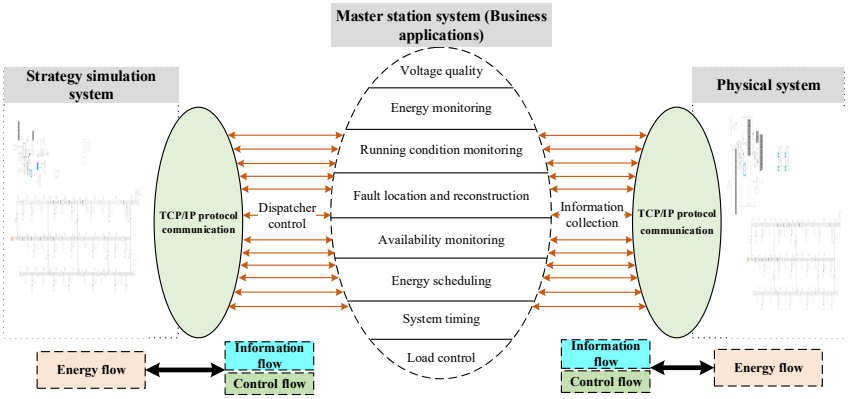


Figure 2. Microgrid cyber-physical systems and business integration platform architecture.

In the architecture of the microgrid information physics and business integration platform, the entire platform architecture is divided into a strategy simulation system, a main station system, and a physical system. The fusion of communication and control between the strategy simulation system, physical system, and main station system is achieved through the application of information physics technology. The specific fusion method is as follows.

The master station system collects energy information, such as voltage and current, from the physical system via Transmission Control Protocol/Internet Protocol (TCP/IP) protocol communication. As shown in Figure 3, the master station system queries the business application in the business database. Different business applications correspond to different business scenarios and functional instructions. The extracted functional instructions are then scheduled to the strategy simulation system through TCP/IP protocol communication. The strategy simulation system replicates the energy information from the physical system and converts the scheduled functional instructions into sequential control operations executable by the simulation model. The simulation results are transmitted in real time to the master station system via cyber-physical technology. The master station system assesses the usability and stability of the simulation results and then issues the same functional instructions to the physical system to realize the reproduction of the business scenario and optimization of faults.

The simulation architecture of the information, physical, and business integration platform built in this article achieves the integration of upper level business and lower level physical information. The business query method of the main station system can simulate different business applications in real time, and the simulation results of the strategy simulation system will also query the content in the corresponding library. The main purpose is to improve the real-time simulation speed of each scenario, and quickly achieve scenario reproduction and fault optimization. Additionally, in practical microgrid operations, the three-layer simulation approach involving the strategy simulation system, master station system, and physical system reduces the time consumption for fault optimization during the operation of the microgrid, providing technical support for the stable operation of the microgrid.

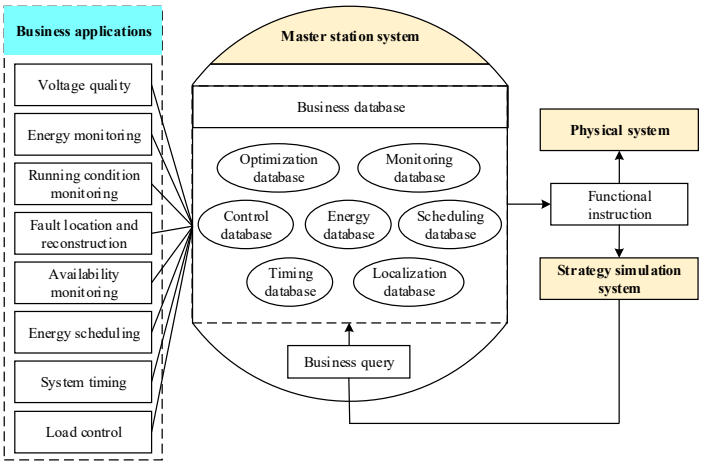


Figure 3. Master station system business query method.

3. Construction of Simulation Model Based on FSM

3.1. Principles of FSM

The FSM is a mathematical model with discrete inputs and outputs, which has advantages in structure and dynamic transformation, providing theoretical support for the integration of information physics and business architecture in simulation platforms.

Figure 4 shows the FSM model of the simulation platform, where FSC is the finite state controller. The interaction between the main station system, strategy simulation system, and physical system can be described through state transitions. The energy and state information of the physical system are transmitted to the input storage band of the finite state machine of the main station through TCP/IP communication protocol in the form of input signals. FSC identifies the state and energy information in the FSM input storage tape, and achieves state transition through instruction conversion, and sends functional command information to the strategy simulation system. If the simulation results are satisfactory, the functional command is returned to the main station system and forwarded to the physical system. The finite state machine is used to simulate the control center of the main station system, modeling the process of receiving state awareness information and outputting functional commands, thereby achieving state transitions.

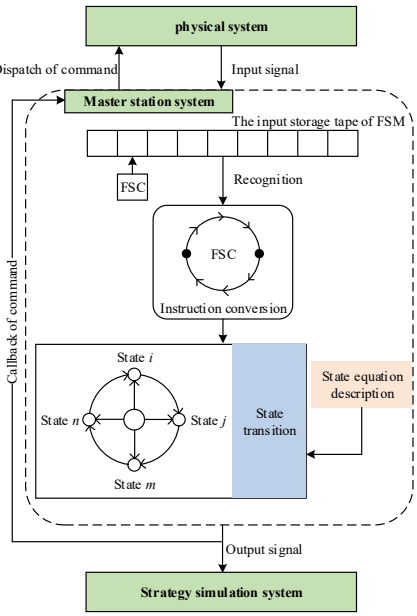


Figure 4. Finite state machine model.

3.2. Mathematical Description of FSM Model

The basic elements of FSM include events, states, actions, and transitions. Events are input conditions for FSM. In a certain state, when an event is triggered, the corresponding action will be executed to transition to another state. A state is a means of describing an object, and all states of an object constitute a set of states, and at any given time, it will only be in one of these states. An action is a response to events. Transitions are state transition functions that enable control over system state transitions. FSM can be represented by a five-tuple:

$$FSM = (S, C, f, S_0, S_n) \tag{1}$$

where S is a finite set of states; C is the collection of events; S_0 is the initial state; S_n is the target state; and f is the state transition function.

$$S_n = f(S_i, C_i) \tag{2}$$

where S_i is the current state; and C_i is the current input event. S_n represents the state that can be reached when the FSM is in state S_i and the event condition C_i is met.

When the state S_n is reached, the corresponding output set is

$$O_n = g(S_n, C_n) \tag{3}$$

where O_n is the output state of the system at time n; g is the output function, indicating the output rules of the system affected by the current state and input events; and C_n is the set of output events.

The state set contains more state information, so the state set is divided into three subsets: physical system, master station system, and strategy simulation system. Each subset represents different states of different systems at different times. Figure 5 shows the basic principle of FSM. When the event is triggered, the current state of the physical system changes. With the change in events and time, the state can transfer between different systems. For example, when the physical system state changes to S_1, with the change in events and time, the state can be transferred to S_2 in the same system or S_2 in the master station system. When the master station system status is S_2, it can be transferred to S_j in the same system or S_j in the strategy simulation system, until the end of all state transitions, including input and output events that trigger state changes.

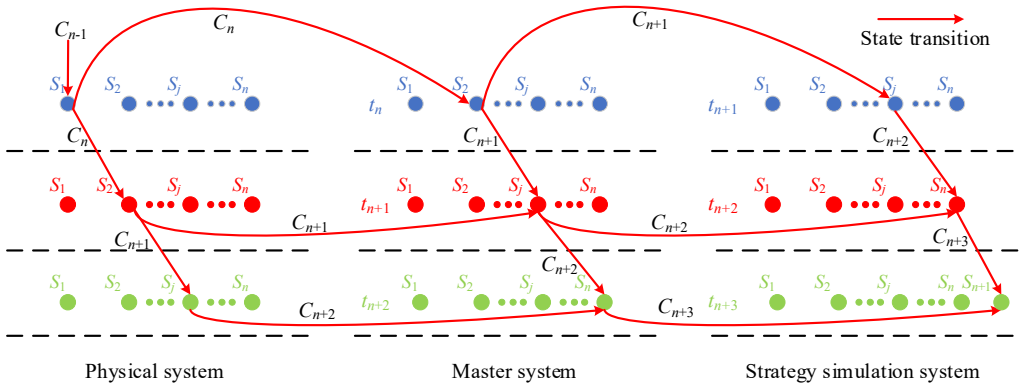


Figure 5. Basic principle of FSM.

FSM exists in the physical system, strategy simulation system, and master station system, which effectively connects discrete information and continuous information through state transition. The status and energy information of the physical system is transmitted to the master station system through the TCP/IP communication protocol. The FSM in the

master station system reads, parses, and re-encodes the information. Then, it is transmitted to the strategy simulation system for discrete simulation. Finally, the optimized instruction information is transmitted to the physical system through the master station system for execution. Details of the TCP/IP communication protocol are as follows:

(1) The TCP/IP communication protocol defines the four-layer framework of network interconnection, as shown in Figure 6. This paper mainly applies the application layer, transport layer, and network layer of the TCP/IP communication protocol. The network layer is responsible for finding a suitable path for the data packets to be sent in the complex network environment. The specific address information is 192.168.1.44 and 192.168.1.140.

(2) The transmission layer carries transmission information, including system number, status, command information, switch information, node voltage, and current information. The transmission layer sends them in the specified order.

(3) The application layer can support user applications. When the application layer is combined with the finite state machine, the FSC is responsible for reading and writing the data of the transport layer. After reading and before writing, it needs to go through the instruction transition and state transition of the finite state machine model.

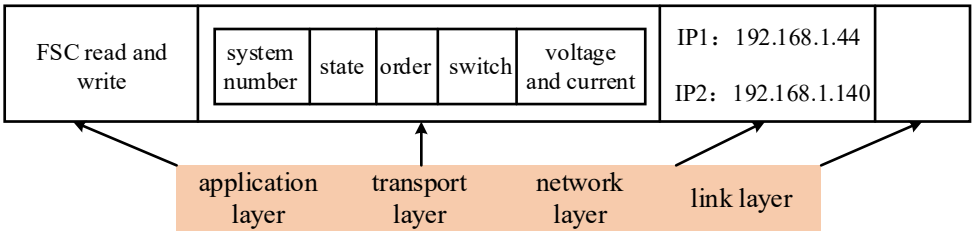


Figure 6. Four-layer framework of TCP/IP communication protocol.

4. Fault Optimization Business State Transition Based on the Simulation Platform

4.1. Defining Fault Optimization State Strategy

FSM are responsible for managing the switching process of system operation status in the integrated simulation platform. When a state transition occurs, corresponding coordination and control strategies need to be developed. These strategies may include controlling state transitions of physical system control units, driving changes in the state of the master station system, or coordinating the actions and execution of the strategy simulation system to ensure overall system coordination and efficient operation. The definitions of the basic operational state control strategies for the integrated simulation platform are shown in Table 2.

Table 2. Definition of state control strategies.

System	System Identifier	State	Communication Information	Strategy Definition
Physical system	0	s_{w_1}	1	initial state
		s_{w_2}	2	data collection state
		s_{w_3}	3	reclosing state
		s_{w_4}	4	fault state
		s_{w_5}	5	FSM communication state
		s_{w_6}	6	waiting state

Table 2. *Cont.*

System	System Identifier	State	Communication Information	Strategy Definition
Master station system	1	s_{z_1}	1	initial state
		s_{z_2}	2	FSM communication state
		s_{z_3}	3	FSM parses state
		s_{z_4}	4	determine the status of the optimization result
		s_{z_5}	5	issue functional command status
Strategy simulation system	2	s_{c_1}	1	initial state
		s_{c_2}	2	FSM communication state
		s_{c_3}	3	FSM parses state
		s_{c_4}	4	simulation execution status
		s_{c_5}	5	simulation result feedback status

The state definition attributes of the physical system, master station system, and strategy simulation system are as follows (the same state will not be further introduced):

(1) The system number of the physical system is 0, and the communication resolution address is located in the first bit of the TCP/IP communication layer. The communication information resolution address of its state is located in the second bit of the TCP/IP communication layer. The specific status attributes are as follows:
   1. Initial state: The physical system is powered on and initialized.
   2. Data collection state: The energy information of each node in the topology is monitored at all times, including current information and voltage information.
   3. Recloser state: In case of a fault, the physical system will initiate the reclosing operation first and solve the fault problem separately in the physical system.
   4. Fault state: After a reclosing failure, the physical system is defined as a fault state.
   5. Finite state machine communication state: The state definition of a finite state machine in a physical system that interacts with the main station system, and can exchange communication layer information through the TCP/IP protocol.
   6. Waiting state: The physical system is waiting for instruction information optimized by the main station system fault.

(2) The series number of the main station system is 1, and the communication resolution address is located in the first bit of the TCP/IP communication layer. The communication information resolution address for its status is located in the second bit of the TCP/IP communication layer. The specific status attributes are as follows:
   1. Finite state machine communication state: The state definition of the finite state machine in the main station system when it interacts with the physical system and policy simulation system, and can exchange communication layer information through the TCP/IP protocol.
   2. Finite state machine parsing state: When information exchange occurs between the physical system and the main station system, it parses the TCP/IP protocol communication layer. The parsing method is to copy the TCP/IP protocol communication layer information into the input storage tape of FSM. FSC will identify each storage tape based on its location and correspond the identified content to the optimization library in FSM. The optimization library will determine the state transition and output the content of the TCP/IP protocol communication layer.
   3. Judging-the-optimization-result state: The simulation results of the main station system's multi-directional processing strategy simulation system, such as simu-

lation time, solution consumption time, voltage deviation, voltage mean square error, and number of switch actions, are judged.

4. Issue functional instruction state: Instruction information with good performance is issued to the physical system.

(3) The system number of the strategy simulation system is 2, and the communication resolution address is located at the first bit of the TCP/IP communication layer. The communication information resolution address for its status is located at the second bit of the TCP/IP communication layer. The specific status attributes are as follows:

1. Simulation execution status: Execute parsed instruction information and simulate different optimization paths.
2. Simulation result feedback status: The strategy simulation system feeds back the simulation results to the main station system and transitions the state to the initial state.

The state definition provides partial data for the TCP/IP communication layer, facilitating the identification of system numbers and states by different systems, and providing communication references for the subsequent transmission and execution of command information, switch information, voltage, current, and power information.

4.2. Defining Fault Optimization State Transition and Communication

In the simulation platform, when a fault occurs at a certain node on the physical system side, fault optimization is performed through the following steps:

(1) The state transition of the physical system in the simulation platform is shown in Figure 7. The physical system initially resides in the initial state. When a significant change in the monitoring node's current occurs, the state transitions to the data collection state, and real-time current information from each node is collected. Then, using a difference-based method, the fault node on the primary side is identified, and the switches on both ends of the fault node are disconnected.

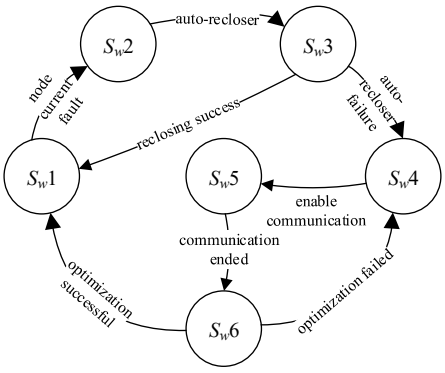


Figure 7. Physical system state transition process.

(2) After the fault node is determined, the state transitions to the reclosing state. The physical system then initiates the reclosing operation and re-evaluates the processed current difference. If the current state is normal, the fault is cleared; if the reclosing fails, the fault information is locked, and the state transitions to the fault state.

(3) In the fault state, the physical system uploads the system ID, current state, fault node ID, instruction information, switch information, node voltage, and current information (collectively referred to as program variable parameters) through TCP/IP communication to the master system. After the information is transmitted, the system then transitions to the waiting state.

(4) The state transition of the master station system in the simulation platform is shown in Figure 8. Initially, the master station system is in the initial state. When the second position of the program variable parameters received from the physical system equals 4, the state transitions to the finite state machine communication state, where the received information is parsed. At this point, the state transitions to the finite state machine parsing state, where the fault node is used to query the corresponding instruction and switch information. The specific path information for fault optimization is shown in Table 3. Upon successful parsing, the state transitions back to the finite state machine communication state, where communication with the strategy simulation system occurs.

Table 3. Fault optimization library.

Node	**1–3**	**4–6**	**7–9**	**10**	**15–17**	**18–20**	**21**	**24–25**	**26–28**	**29–32**	**11–14, 23, 33**
Path	L_1	L_1–L_6	L_1–L_3	L_1	L_1	L_1–L_2	L_1	L_1	L_1–L_3	L_1	off-grid
Switch (k_1–k_6)	100000	000100 010000 001000 011000 010100 001100	001000 000010 000001	000001	000100	000010 ——— 000001	000001	100000	010000 001000 011000	001000	000000

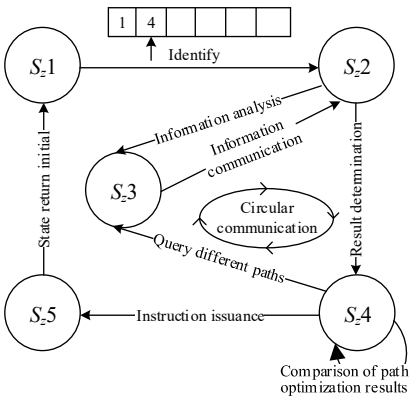


Figure 8. Master station system state transition process.

(5) In the simulation platform, the state transition of the strategy simulation system is shown in Figure 9. The strategy simulation system is initially in the initial state. When it receives the program variable parameter with the second position as 2 from the master station system, the state transitions to the finite state machine communication state and begins parsing the received information. At this point, the state transitions to the finite state machine parsing state, and the parsing process is as follows: a. Copy the fault information of the physical system based on the fault node number; b. Modify the topology based on switch and instruction information, and optimize different paths. During the execution of related instruction information, the state of the strategy simulation system is the simulation execution state. After the simulation concludes, the state transitions to the simulation result feedback state, where the optimized program variable parameters (mainly voltage and current information) are uploaded to the master station system.

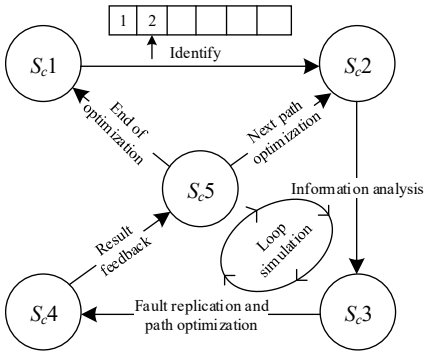


Figure 9. Strategy simulation system state transition process.

(6) When the master station system in the finite state machine communication state receives the result feedback information from the strategy simulation system, the state transitions to the judgment of optimization results state. The system then evaluates and records the feedback information for optimization results. At this point, the first fault optimization is completed. The master station system will continue to communicate in a loop with the strategy simulation system, based on different path optimization information from the optimization library, until all path optimizations are simulated and completed.

(7) Similarly, the strategy simulation system in the simulation result feedback state will continue to identify the program variable parameter in the second position from the master station system and continue performing the loop simulations until all path simulation results are completed. All feedback information will then be uploaded, and the final state transitions to the initial state.

(8) After the final path optimization result feedback, the master station system will perform a determination based on the mean square deviation and simulation time for all path optimization information. The optimal result will be selected, and the path optimization information with the best result will be sent to the physical system. The state will then transition to the initial state.

(9) The physical system, in the waiting state, will execute the best path information sent by the master station system, control the switches for fault optimization, and, after a successful optimization, the state will transition back to the initial state.

5. Simulation Experiment Verification and Analysis

To validate the usability of the proposed integrated simulation platform, a semi-hardware-in-the-loop simulation system, as shown in Figure 10, is constructed. The system mainly consists of a rapid control prototype (RCP), hardware-in-the-loop (HIL), and an upper computer. The RCP model is PXIe-1071, Intel i3 dual core CPU2.6GHz per core, equipped with NI-PXIe-7846R board; the HIL model is PXIe-1082, Intel i7 quad core CPU2.6GHz per core, equipped with NI-PXIe-7858R board; the upper computer has an i7-7700 quad core CPU with a frequency of 1.6 GHz per core and a RAM of 16.0 GB.

The upper computer is used to install the application software StarSim RCP (version: 4.6.9.0) and the HIL application software StarSim HIL (version: 4.6.9.0) for RCP. The microgrid topology model is downloaded from the upper computer to the HIL system. The control module, compiled with Simulink (version: 2018a)-generated .tlc code, is deployed on the RCP, with the physical system and the strategy simulation system running on HIL, and the master station system running on the RCP. After configuring network addresses within the same local area network, data can be exchanged directly between the RCP and HIL through analog and digital ports. Since all simulations on both RCP and HIL are performed with a time step of 100 μs, and considering the fiber-optic communication delay

on the microsecond level, the signal delay through the analog port is approximately 200 µs. The microsecond-level delay is neglected, and the voltage signals are measured using an oscilloscope. Due to the IO interface's signal communication limit of 10, the voltage signal is scaled down by 1000 times when passing through the RCP's IO port. After passing through HIL, the voltage signal is restored to 1000 times its original value.

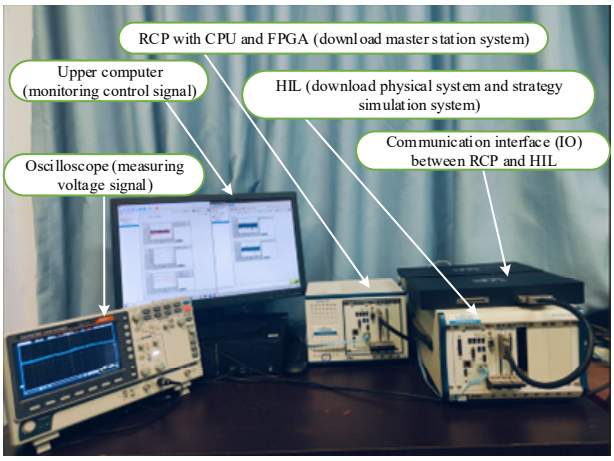


Figure 10. Semi-hardware-in-the-loop simulation system.

5.1. Simulation Experiment Analysis

The physical system simulates a real power grid, demonstrating grid faults through physical system failures. As shown in Figure 11, a new microgrid topology model with an IEEE 33-node, 10 kV power source is established. Under normal operation, the switches g_i on both sides of the nodes are closed, while the optimization switches k_i (represented by the dashed lines) are open. In the fault state, the optimization switches and node switches can operate according to the optimized switch command information. Based on the communication strategy and state transitions of the integrated simulation platform, a short-circuit fault is created at node 26, while the remaining nodes are in a normally connected state, and a simulation analysis is conducted.

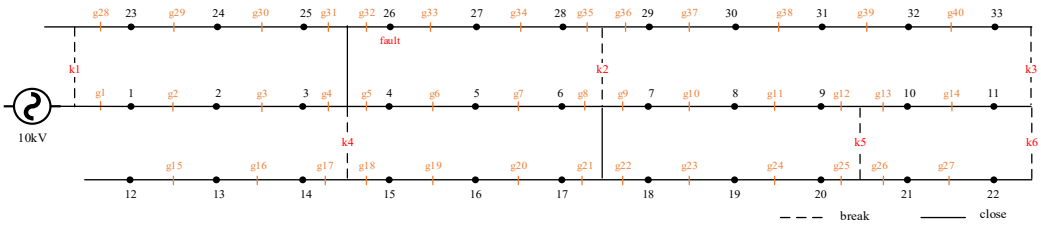


Figure 11. IEEE 33 node novel microgrid topology.

Figure 12 shows the state transition results of the physical system, master station system, and strategy simulation system within the integrated simulation platform. Based on the fault optimization state strategy proposed above, when the physical system is in a fault state, the master station system receives the program variable parameters from the physical system, performs parameter analysis, and engages in a cyclic communication with the strategy simulation system. A total of three path optimization simulations are conducted. Taking the time point 15 as an example, the strategy simulation system is in the simulation result feedback state, the master station system is in the judgment of optimization result state, and the physical system is in the waiting state. At this point, after the master station system concludes the optimization result judgment, it sends the third path optimization command information to the strategy simulation system, which, upon

receiving it, continues executing the path optimization until all three path optimization simulations are completed. Throughout this interval, the physical system remains in the waiting state. The physical system, master station system, and strategy simulation system in the integrated simulation platform execute according to the strategy and communication format, with the simulation results fully aligning with the previously described outcomes. This supports the inference of the availability of the simulation platform in executing the strategy.

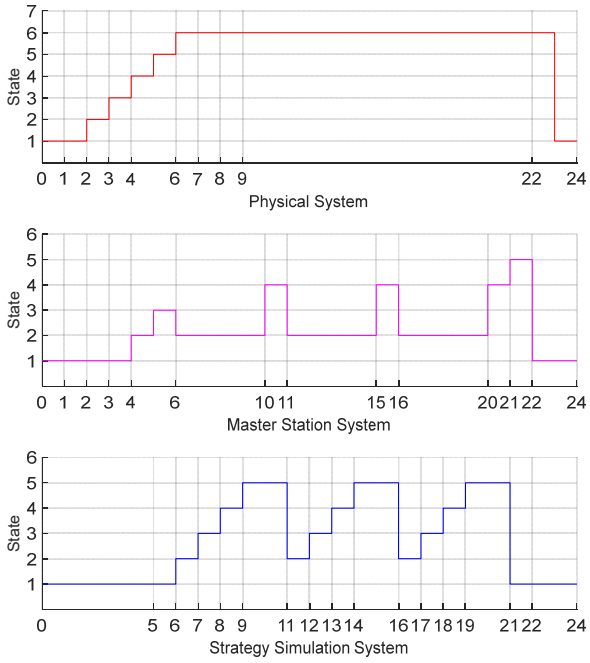


Figure 12. State transition process of simulation platform.

5.2. Conclusion Analysis

Due to the short-circuit fault occurring at node 26, the voltage at node 27 was collected for result analysis. Figure 13 shows the voltage variation throughout the entire simulation process at node 27. The oscilloscope probe has a 1000:1 ratio. Under normal conditions, the voltage at node 27 is 7.75 kV, and it can be observed that there are a total of four voltage changes.

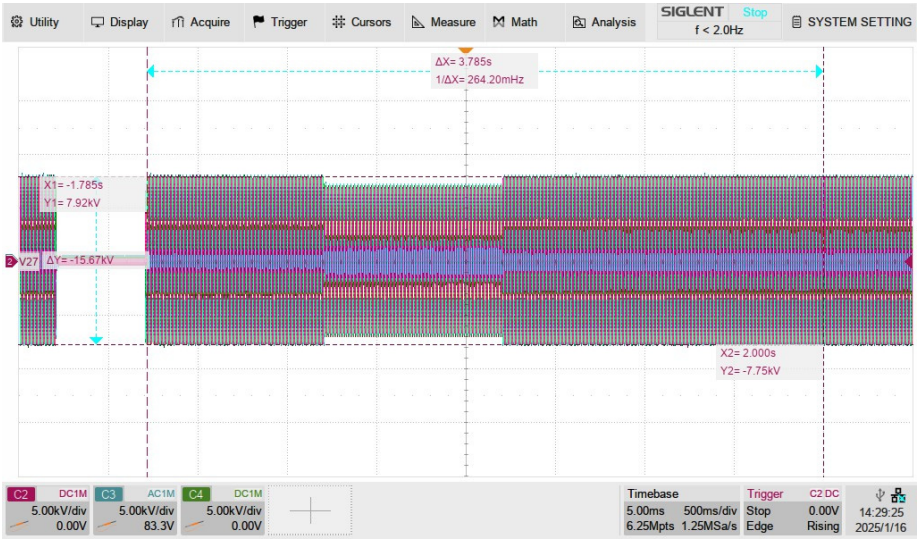


Figure 13. The voltage variation diagram of the whole process of the 27-node simulation.

The first change was caused by a short-circuit fault at node 26. Figure 14 shows that the voltage of node 27 is basically kept at 0 when a short-circuit fault occurs at node 26. The remaining changes are due to the optimization of simulation platform faults. The first path optimization switch signal k_i = 010000, and the switch acts 3 times. Figure 15 shows that the voltage at node 27 has recovered to about 7.75 kV, basically completely recovered. The second path optimization switch signal k_i = 001000, and the switch acts 3 times. The voltage at node 27 is restored to about 6.75 kV, which is significantly different from the initial voltage at node 27. The third path optimization switch signal k_i = 011000, and the switch acts 4 times. Figure 16 shows that the voltage at node 27 recovered to about 7.75 kV, basically completely recovered.

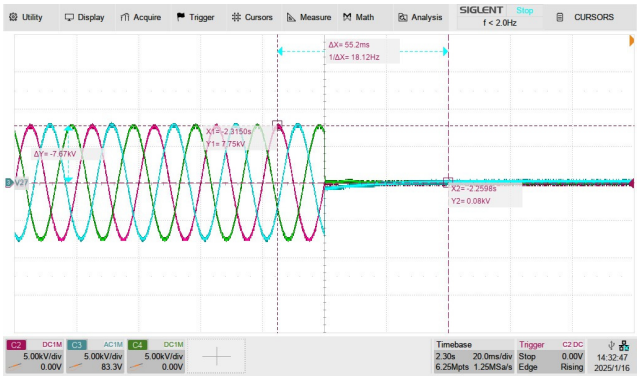


Figure 14. Voltage variation diagram of node 27 when short-circuit fault occurred.

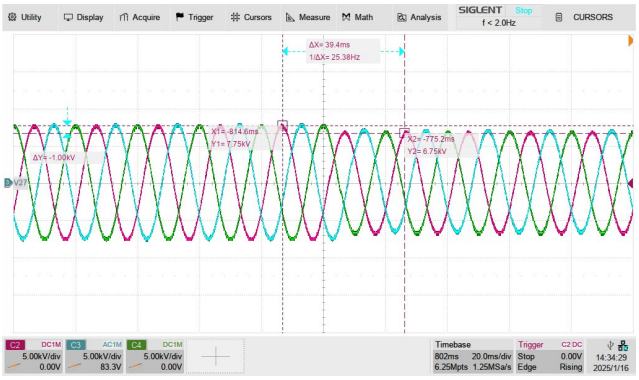


Figure 15. Node 27's first and second optimized voltage diagram.

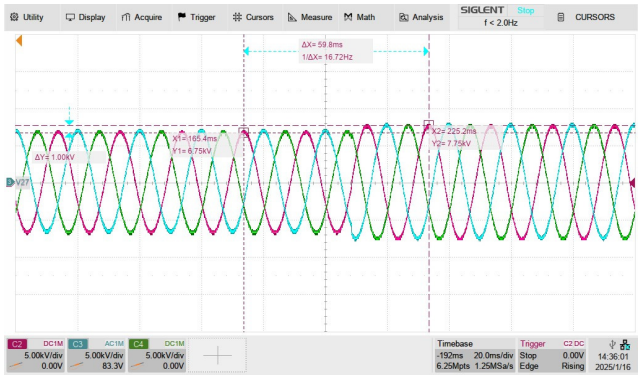


Figure 16. Node 27's second and third optimized voltage diagram.

A comparative analysis was conducted with existing methods in terms of simulation time and optimal path selection while ensuring the similarity of microgrid topology. Table 4 shows

the comparison results of optimization time between the proposed method and C-ADMM-A algorithm, C-ADMM-F algorithm, CADMM + SA algorithm, QA-ADMM-A-1 algorithm, and QA-ADMM-A-2 algorithm [26] on the IEEE-33 microgrid topology. The fault optimization time of the proposed method in this paper is 0.512 s, which consumes the least time compared with the traditional optimization strategy, and is reduced by about 16–86.6%.

Table 4. Comparison of solution time.

Strategy		Time Consumption for Fault Optimization Solution (s)
Traditional optimization strategies	C-ADMM-A	0.609
	C-ADMM-F	3.829
	CADMM + SA	2.830
	QA-ADMM-A-1	2.044
	QA-ADMM-A-2	0.725
The method proposed in this article		0.512

The voltage mean square deviation, average voltage deviation, and switching action times are taken as the optimization objectives to select the best path.

Table 5 shows the comparison results of the objectives after fault optimization in the example:

(1) When the main objective is to minimize the voltage mean square deviation and the average voltage deviation, while auxiliary objective is to minimize the number of switching actions, the first recovery path is optimal;
(2) When the only objective is to minimize the number of switching actions, the second recovery path is optimal;
(3) When taking the minimum voltage mean square deviation, the minimum average voltage deviation, and the minimum number of switching actions as the same weight objectives, the third recovery path is optimal.

Table 5. Comparative results of the objectives.

Objectives / Path	Voltage Mean Square Deviation (kV)	Average Voltage Deviation (%)	Switching Action Times
First path	0.02	0.26	3
Second path	0.83	10.71	3
Third path	0.03	0.39	4

6. Conclusions

The efficient operation of microgrids urgently requires the deep integration of information physics technology and business to achieve the reproduction of source load dynamic regulation scenarios. In response to this demand, this article has made the following main contributions:

(1) A CPS-based microgrid simulation platform is proposed, which integrates information physics technology and business architecture to achieve real-time simulation and reproduction of business scenarios. In theory, it can be connected to the main control system to achieve state decision-making and control.
(2) The fault optimization time of the proposed platform in this paper is 0.512 s, which consumes the least time compared with the traditional optimization methods, and is reduced by about 16–86.6%.
(3) The proposed platform can design different state transition strategies according to different business. Taking fault optimization business as an example, the best path

can be selected through state transition, and the optimal fault recovery of the physical system can be achieved through communication and real-time control.

The proposed platform can be applied to real-time simulation of microgrids with different topologies and scenarios, such as fault optimization, fault location, energy scheduling, and load control. However, reproducing multiple scenarios will lead to a significant increase in dimensionality, making it impossible to achieve real-time simulation and having certain limitations. This is also the future research direction of the platform.

Author Contributions: Conceptualization, D.J. and X.Y.; methodology, D.J.; validation, K.Y., X.L. and W.D.; formal analysis, W.S.; investigation, K.L.; resources, D.J.; data curation, X.Y.; writing—original draft preparation, K.Y.; writing—review and editing, X.L.; project administration, D.J.; funding acquisition, D.J. All authors have read and agreed to the published version of the manuscript.

Funding: This research was funded by the Science and Technology Project of State Grid Corporation of China "Research on the key technology of modeling and simulation analysis of peer-to-peer distribution system", grant number: (5400-202355767A-3-5-YS).

Data Availability Statement: Restrictions apply to the availability of these data. Data were obtained from China Electric Power Research Institute Co., Ltd.; they are limited and are available from the authors with the permission of China Electric Power Research Institute Co., Ltd.

Acknowledgments: We would like to express our gratitude to all the reviewers and editors for providing valuable advice.

Conflicts of Interest: Authors Dongli Jia, Xiaoyu Yang, Wanxing Sheng, Keyan Liu were employed by the company China Electric Power Research Institute Co., Ltd. The remaining authors declare that the research was conducted in the absence of any commercial or financial relationships that could be construed as a potential conflict of interest. The company had no role in the design of the study; in the collection, analyses, or interpretation of data; in the writing of the manuscript, or in the decision to publish the results.

References

1. Hirokazu, I.; Honoka, D.; Soshi, S.; Hidehiko, T.; Yoshikiyo, H.; Takato, N.; Nobuyoshi, N. Enhancing understanding of pressure drop in carbon porous electrodes for vanadium redox flow batteries. *J. Energy Storage* **2023**, *73*, 109066.
2. Yang, Y.; Lu, Q.; Yu, Z.; Wang, W.; Hu, Q. Multi-Type Energy Storage Collaborative Planning in Power System Based on Stochastic Optimization Method. *Processes* **2024**, *12*, 2079. [CrossRef]
3. Yang, Q.M.; Li, G.F.; Bie, Z.H.; Wu, J.Y.; Lin, C.F.; Liu, D.F. Coordinated Power Supply Restoration Method of Resilient Urban Transmission and Distribution Networks Considering Intermittent New Energy. *High Volt. Eng.* **2023**, *49*, 2764–2774.
4. China National Knowledge Infrastructure. Available online: https://kns.cnki.net/kcms2/article/abstract?v=_pLk7jldQwhLeziox4zGOk3D4UsyyRQEE1hIx3i7AKGHnjuAiWUSpyijOuUPM7h40Dxt0bdJFTPk0eje3PR06M5YpzwlcQsVnHfa6GxLD2AYByXu_MYWaInYy8oJSceNUvE1aDw8DLWKejnJMw6dV7ghGGGXW3LY0Ukz74LYc5snz-Id5gUPCQISm5VMFMP3&uniplatform=NZKPT&language=CHS (accessed on 15 November 2024).
5. Yang, H.; Yin, B.; Meng, K.; Yu, H.; Zhou, N.; Xu, Z. Distributed Robust Optimal Scheduling of the New Interconnected Power System with the Inter-province and Intra-province Considering Moment Uncertainty of Source Load Power. *Electr. Power Constr.* **2023**, *44*, 98–110.
6. Yang, L.; Huang, Z.H.; Chen, J.H.; Zheng, D.L.; Hong, M.Z.; Liu, J.X. Optimal Stability Analysis of DC Microgrid Based on Crisscross Optimization Algorithm. *High Volt. Eng.* **2023**, *49*, 4632–4641.
7. Zhang, J.M.; Ouyang, S.; Wu, H.; Xin, X.; Huang, Y. Optimal configuration of grid-side energy storage considering reliability and operation economy of distribution network. *Electr. Power Autom. Equip.* **2024**, *44*, 62–68+85.
8. Li, L.J.; Xu, Y. Flexible DC distribution network fault location method based on beetle swarm optimization algorithm. *J. Phys. Conf. Ser.* **2023**, *2625*, 012001. [CrossRef]
9. Dong, G.C.; He, C.; Liu, X.; Nan, L.; Liu, T.Q.; Zhang, Y.Q. Coordinated recovery method of post-disaster distribution network cyber-physical system considering network reconstruction and emergency resources. *Electr. Power Autom. Equip.* **2024**, *44*, 106–113.
10. China National Knowledge Infrastructure. Available online: https://kns.cnki.net/kcms2/article/abstract?v=_pLk7jldQwiDoWzfs8RAyxeeZIEbbJjLQVSuuh_uNazaRRKP2Arr2tjSEATWlpfOWbM5EqYDlxZBo0ubasdjCpUZu3Q_fuC3Gql4

Lhkt6Wfr6MARMB4abRS1u76D7pPaiPpo3kamPX7kqCBcusN0Ky-QfX6gRMpbXWWKWsoOTT23WVHvr5GYHvTvW9q3Lh4f&uniplatform=NZKPT&language=CHS (accessed on 9 October 2024).

11. Li, H.Z.; Guo, X.C. Reliability Evaluation of Cyber-physical System of Distribution Network Based on Petri Net. *Power Syst. Technol.* **2023**, *47*, 347–359.
12. Pang, Q.L.; Han, S.Y.; Zhou, T.; Zhang, F.; Jiao, X.G.; Wang, Y.Q. False Data Injection Attack Detection of Cyber-physical Power System Based on ASRUKF and IMC Algorithms. *Grid Anal. Study* **2024**, *52*, 111–118.
13. Chen, L.J.; Wang, B. Disaster recovery strategies for cyber-physical systems considering the Interdependence. *Electr. Power Syst. Res.* **2024**, *232*, 110397. [CrossRef]
14. Liu, Y.L.; Feng, H.N.; Hatziargyriou, N.D. Multi-stage collaborative resilient enhancement strategy for coupling faults in distribution cyber physical systems. *Appl. Energy* **2023**, *348*, 121560. [CrossRef]
15. Yang, Y.; Yang, P. The Hierarchical Modeling Approach for Centralized Control Microgrid Cyber Physical System. *Proc. CSEE* **2022**, *42*, 7088–7102.
16. Zheng, H.K.; Lv, T.T.; Sun, Y.W.; Li, Y.J.; Yu, K.D. Reliability Analysis of Integrated Energy Cyber Physical System Considering Information Equipment Failure. *High Volt. Eng.* **2022**, *48*, 3078–3087.
17. He, H.; Liang, Y.; Liu, K.Y.; Weng, Y.H. Active Distribution Network Voltage Control Method Considering Communication Interruption. *Power Inf. Commun. Technol.* **2022**, *20*, 1–10.
18. Huang, Z.; Liu, D.; Chen, G.H.; Weng, J.M.; Yin, H.Y.; Wang, Z. The evolution mechanism of the cyber-physical cascading failure of power distribution system based on event-driven. *Electr. Power Eng. Technol.* **2022**, *41*, 2–13.
19. Anant, M.T.; Dusmanta, K.M. RBFNN assisted transient instability-based risk assessment of cyber-physical power system. *Int. J. Electr. Power Energy Syst.* **2022**, *137*, 107787.
20. Zhang, J.; Yang, T.; Ji, H.; Li, W. Optimal locating method of edge computing device in cyber physical distribution system. *Energy Rep.* **2022**, *8*, 684–694. [CrossRef]
21. Fang, Y.; Tang, X.; Tang, L.; Chen, Y.; Wang, W. Local Evolution Model of the Communication Network for Reducing Outage Risk of Power Cyber-Physical System. *Energies* **2022**, *15*, 7876. [CrossRef]
22. Yang, Z.; Jia, W.; Xu, B.W.; Min, X.; Zhao, F.L.; Xu, L. Error Proof Control Method for Real-time Power Dispatching Based on Finite State Machine. *Electr. Eng.* **2023**, *12*, 176–178+182.
23. Zhou, H.B.; Yang, J.; Huang, L.S.; Song, D.R.; Chen, X.J.; Dong, M. Double-vector Model Predictive Control Strategy of Three-level Inverter Based on Finite State Machine. *Autom. Electr. Power Syst.* **2023**, *47*, 155–164.
24. Zhong, M.H.; Tong, X.Q.; Liu, X.H. A new fast PWM modulation strategy for power electric converter based on finite set state machine theory. *Energy Rep.* **2023**, *9*, 90–96. [CrossRef]
25. Liu, K.Y.; Li, Z.; Jia, D.L.; Ye, X.S. Multi-flow Fusion Simulation Engine for New Distribution Network Based on Finite State Machine. *High Volt. Eng.* **2023**, *50*, 4826–4836.
26. Fu, W.; Xie, H.; Wang, H.; Chen, C.; Bie, Z. Post-Disaster Topological Reconfiguration Approachfor Distribution Networks Using Hybrid Quantum-Classical Algorithm. *J. Xi'an Jiaotong Univ.* **2025**, *59*, 1–16.

Disclaimer/Publisher's Note: The statements, opinions and data contained in all publications are solely those of the individual author(s) and contributor(s) and not of MDPI and/or the editor(s). MDPI and/or the editor(s) disclaim responsibility for any injury to people or property resulting from any ideas, methods, instructions or products referred to in the content.